Title

Radiographs acquired before total hip replacement in dogs underestimate femoral canal flare and misjudge trochanteric overhang.

Authors

Bae, Sohee

Marcellin-Little, Denis J

Pritikin, Ridhdi

et al.

Publication Date

2025-04-14

DOI

10.2460/ajvr.25.02.0045

AJVR

AVMA

Radiographs acquired before total hip replacement in dogs underestimate femoral canal flare and misjudge trochanteric overhang

Sohee Bae, DVM, MS; Denis J. Marcellin-Little, DEDV, DACVS, DACVSMR*; Ridhdi Pritikin, BS; Tanya C. Garcia, MS

JD Wheat Veterinary Orthopedic Research Laboratory, School of Veterinary Medicine, University of California-Davis, Davis, CA

*Corresponding author: Dr. Marcellin-Little (djmarcel@ucdavis.edu)

Objective
To compare measurements of canal flare index (CFI) and greater trochanter overhang (TrO) from ventrodorsal (VD) and craniocaudal horizontal beam (CCHB) radiographic views to measurements from contemporaneously acquired CT scans and to evaluate the impact of size, age, radiographic view, severity of osteoarthritis, hip subluxation, and femoral rotational malposition on CFI and TrO measurement accuracy.

Methods
This was a retrospective study of femurs imaged from June 28, 2018, through March 27, 2023. The CFI and linear TrO index measured from VD and CCHB radiographs and from CT-derived surface renderings of the femur prepared with −10°, −5°, 0°, +5°, and +10° of rotation using computer-aided design software were compared.

Results
80 femora from 43 dogs were included. Radiographs measured CFI with errors > 0.2 in 81% of VD views and 77% of CCHB views and yielded linear TrO measurements with errors > 20% of canal radius in 75% of VD and 74% of CCHB views. The TrO grade was incorrect for 44% of femurs on VD views and 30% of femurs on CCHB views. Internal femoral rotation of 10° significantly influenced CT measurements of CFI and TrO. Severity of osteoarthritis and hip subluxation did not influence measurements.

Conclusions
Measurements of CFI and TrO from VD and CCHB views are inaccurate relative to CT measurements.

Clinical Relevance
Radiographic measurements underestimate CFI and poorly predict TrO. A CT of the femur should be considered when accurate measurements of CFI and TrO are sought, particularly for femurs with abnormal geometry.

Keywords: total hip replacement, canal flare, trochanteric overhang, computer-aided design, dog

Total hip replacement (THR) is used to manage debilitating problems of the hip joint, such as osteoarthritis (OA) secondary to hip dysplasia, luxation, and fracture managed unsuccessfully without surgery or with other surgical procedures.[1–3] Cementless THR gained popularity over time, potentially due to concerns about aseptic loosening after cemented THR.[4–6] The long-term stability of cementless THR implants often relies on bone ingrowth into prosthetic components. Bone ingrowth requires relative motion between the bone and implant in the early postoperative period to be small (< 20 µm).[7] Stem stability within the femur is enhanced when the stem is fitted to the bone. Press fit relies on circumferential contact with cancellous bone and canal fill. Canal fill is more easily and safely obtained when canal flare approximates the flare of the stem and when the stem is aligned with the long axis of the proximal portion of the femur.[8,9] However, longitudinal stem alignment may be challenging when the greater trochanter overhangs the canal.[10,11] For these reasons, canal flare and trochanteric overhang (TrO) are routinely evaluated when planning cementless THR.[11,12] Radiographic views, however, are subject to distortion.[13] It is unclear whether the radiographic assessment of canal flare and TrO in the dog femur is accurate and what factors influence that accuracy.

The purpose of this study was to evaluate the accuracy of the radiographic assessment of canal

Received February 10, 2025
Accepted March 29, 2025
Published online April 14, 2025

doi.org/10.2460/ajvr.25.02.0045

flare and TrO in dogs by comparing radiographic measurements to CT measurements in 2-D and 3-D. Measurements from controlled rotational femoral malposition of 3-D renderings of the femur were also assessed as it is one of the common radiographic artifacts. The study also aimed to evaluate the effects of hip disease severity on the accuracy of radiographic assessment of canal flare index (CFI) and TrO index. We hypothesized that measurements of CFI and TrO index and grade from ventrodorsal (VD) and craniocaudal horizontal beam (CCHB) radiographic views are inaccurate relative to nonrotated CT renderings. Here, CFI accuracy is defined as a difference between radiographic and CT measurements < 0.20,[12] an accuracy threshold selected based on previously reported[14–16] CFIs of dog femurs. A CFI error of 0.20 would lead to the misclassification of the femoral morphology for approximately 25% of dogs. The accuracy of TrO was defined as a difference between radiographic and CT measurements of TrO < 20% of canal radius or as having the same TrO grade.[11] We hypothesized that CCHB views are more accurate than VD views to measure CFI and TrO. We hypothesized that the accuracy of CFI and TrO is less when the femur is viewed with 5° or 10° internal or external rotation than when the femur is viewed without rotation. We also hypothesized that increased OA or hip subluxation severity negatively impacts the accuracy of radiographic assessment of CFI and TrO index. To conduct this study, radiographs and CT scans of femurs acquired contemporaneously in dogs presented for the management of chronic hip pain were analyzed.

Methods

Sample

This retrospective study used a sample of convenience. Dogs presented to the University of California-Davis Veterinary Medical Teaching Hospital from June 28, 2018, through March 27, 2023, were eligible for inclusion if a CT scan of 1 femur or both had been acquired in addition to radiographs. The CT scan and radiographs were acquired under IV sedation with butorphanol (0.2 mg/kg) combined with dexmedetomidine (approx 0.005 mg/kg). Dexmedetomidine was dosed to effect so that dogs could be positioned for the CT scan and radiographs without eliciting a pain response to hip extension. In our setting, a CT is acquired in addition to radiographs when clinicians perceive the need to accurately evaluate bone size or geometry when planning THR. Dogs were excluded if the CT did not include a complete femur, if motion artifacts were present, or if > 2 weeks lapsed between CT and radiographs. Signalment (age, breed, sex, and weight) was recorded.

Two-dimensional proximal femoral geometry

The DICOM files of radiographs were imported into a commercially available DICOM reader program (Horos, version 3.3.6; Horos Project) and were anonymized. Measurements of CFI and TrO were collected on VD and CCHB radiographic views using previously reported methods **(Figure 1)**.[11,12] For all radiographic views, the patella was centered over the femoral condyles, and the fabellae bisected the femoral cortices. For the VD view, the x-ray beam was centered on the midline, at the level of the hip joints. For the CCHB view, the x-ray beam was centered on the proximal aspect of the femoral diaphysis. Canal radius was determined at the isthmus. The CFI was the ratio of endosteal width at the lesser trochanter and width at the isthmus.[12] Linear TrO index was calculated by dividing the distance from the medial aspect of the greater trochanter to femoral centerline by the canal radius.[11] Greater linear TrO indices represented less TrO. An index ≥ 1 indicated that TrO was not observed. The TrO was graded using a previously reported method, where the location of the medial aspect of the greater trochanter was lateral to the proximal extension of the lateral femoral cortex (grade 1), within the lateral femoral cortex (grade 2), medial to the lateral cortex but lateral to the femoral anatomic axis (grade 3), or medial to the femoral anatomic axis (grade 4).[11] The severity of OA was scored using the modified British Veterinary Association/Kennel Club scheme.[17] The maximal OA score was 41. Hip subluxation was calculated as the ratio of the distance between the center of the femoral head and acetabulum divided by the head radius.

Three-dimensional assessment of CFI and TrO

The DICOM files of CT scans were exported into segmentation software (Mimics, version 23.0; Materialise). The femur was separated from the pelvis and tibia and saved as a 3-D surface rendering (*.stl* file). The CT-based 3-D surface rendering of the femur was imported into computer-aided design software (3-matic, version 15.0; Materialise). A mediolateral condylar axis was developed by joining the centers of spheres fitted to the medial and lateral femoral condyles.[18] A frontal plane was established that was parallel to the mediolateral condylar axis and the long axis of the proximal diaphyseal femoral canal (ie, the centerline of a cylinder fitted to the femoral endosteal surface). Sagittal and transverse planes were generated as planes perpendicular to the frontal plane and to each other. Four oblique frontal planes were generated at 5° increments of internal rotation (+5° and +10°) and external rotation (−10° and −5°). A positive rotation represented internal rotation of the femur relative to a fixed sagittal plane (ie, a craniolateral-to-caudomedial oblique frontal plane projection). The medial aspect of the greater and lesser trochanter was marked with points. To measure CFI, a frontal plane sketch and 4 oblique sketches with −10°, −5°, +5°, and +10° of rotation were created. Projections of the femur and trochanteric points were imported into the sketches with outlines of the endosteal and periosteal surfaces of the femur (Figure 1). When outlines were indistinct, a line was fitted to the medial or lateral endosteal surfaces to approximate the outline. Similar to radiographic measurements, CFI was calculated as the ratio of endosteal width and width at the isthmus (the diameter of the cylinder fitted to

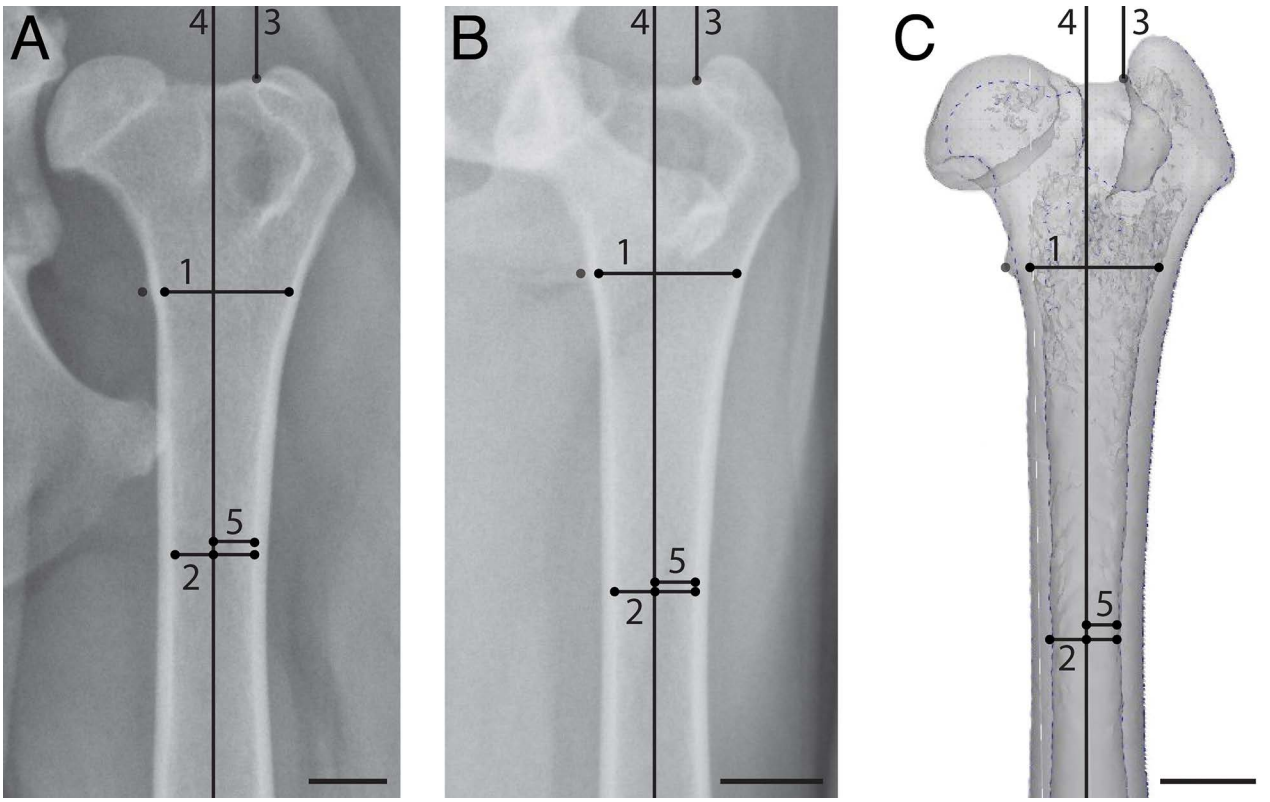

Figure 1—Representative images used to calculate canal flare index (CFI) and linear trochanteric overhang (TrO) index for the right femur of a 9-month-old Border Collie. The images include a ventrodorsal (VD) radiographic view (A), a craniocaudal horizontal beam (CCHB) radiographic view (B), and a CT-derived rendering and sketch of the proximal portion of the femur (C). On these views, CFI is the ratio of endosteal width at the proximodistal midpoint of the lesser trochanter (1) and width at the femoral isthmus (2). The linear TrO index is the ratio of distance from the medial aspect of the greater trochanter (3) to the anatomic axis of the proximal portion of the femur (4) and the radius of the canal (5). In the current study, measurements of CFI and TrO index from VD and CCHB views and from CT-derived renderings acquired contemporaneously from 80 femurs from 2018 through 2023 were compared using measurements from CT-derived renderings as the gold standard. For the femur shown, CFI (endosteal width/width at isthmus) was 1.70 (15.44/9.07 mm) on the VD view, 1.70 (13.6/8.02 mm) on the CCHB view, and 1.99 (13.55/6.81 mm) on the CT-derived sketch. The linear TrO index was 0.57 on the VD view, 1.11 on the CCHB view, and 1.12 on the CT-derived sketch. Scale bars = 1 cm.

the canal).[12] When endosteal outlines were not visible due to severe bone sclerosis, measurements of CFI were not collected.

The extent of TrO was evaluated using 3 methods. Two methods (linear TrO index and TrO grade) were identical to the measurements from radiographs. A third method was based on the volume of the greater trochanter intersecting a proximal extension of the canal (volumetric TrO index). To measure the volumetric TrO index, the greater trochanter was separated from the femur at its distal aspect. To consistently determine the location of the distal aspect of the greater trochanter, the transverse plane was duplicated. The duplicate transverse plane was moved to the proximal aspect of the greater trochanter. The transverse plane was duplicated again. That duplicate plane was translated distally by a length equal to the medullary diameter. The greater trochanter was located between the 2 planes. Bone not belonging to the greater trochanter (ie, femoral head and ossum collis femoris) was deleted. The volume of greater trochanter located within the proximal extension of the medullary cylinder was measured using a Boolean intersection operation **(Figure 2)**. That volume was indexed by dividing the TrO overhang volume by the (canal radius)^3.

Statistical analyses

The normality of distributions was assessed using Shapiro-Wilk tests. Data were considered normally distributed when $W > 0.90$ and $P > .05$. Imaging modalities were compared using ANOVA, with the limb as a random effect and bodyweight as a fixed effect. Pairwise comparisons were made using Tukey honestly significant difference post hoc tests. To measure method reliability, intraclass correlation coefficients (ICCs) were calculated for CFI and linear and volumetric TrO indices.[19] Intraclass correlation coefficient values < 0.5 represented poor consistency, values ≥ 0.5 and < 0.75 represented moderate consistency, values ≥ 0.75 and < 0.9 represented good consistency, and values ≥ 0.90 represented excellent consistency.[20] Linearly weighted κ coefficients were calculated to compare TrO grades from radiographic views and CT renderings in the frontal plane. For these comparisons, $\kappa < 0$ indicated

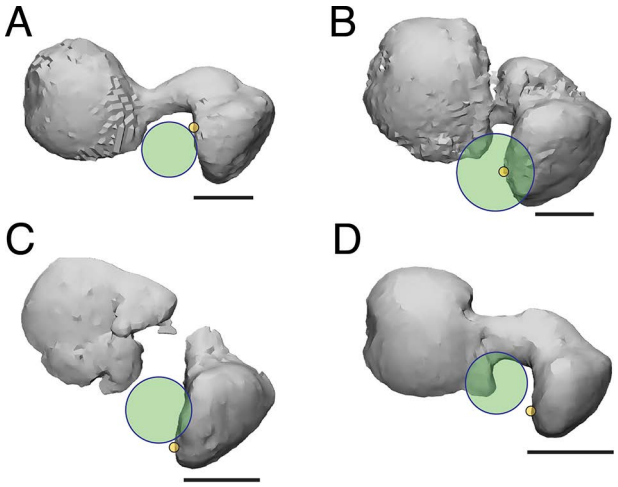

Figure 2—Proximal views of 4 CT-derived renderings of the femurs as described in the legend of Figure 1. The 4 dogs with hip dysplasia evaluated for total hip replacement included a 32-month-old Labrador Retriever weighing 34 kg (A), a 40-month-old German Shepherd Dog weighing 38 kg (B), a 14-month-old Golden Retriever weighing 25 kg (C), and a 9-month-old Border Collie weighing 14 kg (D). Femurs are oriented with their lateral and cranial aspects on the right side and top side of each image, respectively. The circles represent a cylinder fitted to the medullary canal of the proximal portion of the femur. The yellow dots mark the medial aspect of the greater trochanter. The location of the medial aspect of the greater trochanter relative to the medullary canal was determined. The medial aspect of the greater trochanter could be located cranial to the cylinder (A), within the cylinder (B), caudal to the cylinder (C), or lateral (D) to the cylinder representing the canal. For the femur in (A), the canal radius was 4.64 mm, the linear TrO index was 0.72, the TrO grade was 3, and the volumetric TrO index was 0.01. For the femur in (B), those values were 6.59 mm, 0.22, 3, and 0.74. For the femur in (C), those values were 4.32 mm, 0.47, 3, and 0.41. For the femur in (D), those values were 3.59 mm, 1.12, 2, and 0.00. Scale bars = 1 cm.

poor agreement, 0.01 to 0.20 slight agreement, 0.21 to 0.40 fair agreement, 0.41 to 0.60 moderate agreement, 0.61 to 0.80 substantial agreement, and 0.81 to 1 almost perfect agreement.[21] Bias and 95% limits of agreement between radiographic and CT measurements of CFI and TrO indices were determined using Bland-Altman plots.[22] Differences between Bland-Altman plots and differences between the slopes of the regression lines were compared using ANCOVA. Multiple regression with forward selection was done to evaluate the association of the difference between radiographic and CT measurements and other factors (age, bone size, OA score, lateral subluxation index). Correlation between factors was calculated to evaluate collinearity. Linear regression was used to assess the association between radiographic measurements of linear TrO index, CT measurements of linear TrO index, and CT measurements of volumetric TrO index. Regression analysis was used to evaluate the association of bodyweight with CFI and TrO. The CT-based measurements of CFI and linear TrO index collected from renderings at femoral rotations of −10°, −5°, 0°, +5°, and +10° were compared using ANOVA, with the limb as random effect and bodyweight as fixed effect. Pairwise comparisons were made using Tukey honest significant difference post hoc tests. Multiple regression with forward selection was done to evaluate the association of the difference between −10°, −5°, +5°, and +10° femurs and 0° femurs with other factors (age, bone size, OA score, lateral subluxation index). Correlation was run between factors to check collinearity. For all tests, significance was set at $P < .05$.

Results

A total of 82 femurs from 44 dogs were eligible for inclusion. Two femurs from 1 dog were excluded due to motion artifacts, leaving 80 femurs from 43 dogs in the study. Sixty-six femurs were from

Table 1—Canal flare index measurements from 2 radiographic views and from CT scans of 79 femurs from 43 dogs.

Parameter	Viewing method	Mean ± SD	Bias (limits of agreement)*	ICC*	Accuracy*
Endosteal width (mm)	CT, 0° (n = 79)	18.26[a] ± 4.40	—	—	—
	VD (n = 79)	16.50[b] ± 5.06	−1.61 ± 0.66	—	—
	CCHB (n = 70)	16.65[b] ± 4.64	−1.38 ± 0.68	—	—
Diaphyseal width at isthmus (mm)	CT, 0° (n = 79)	9.24[a] ± 2.17	—	—	—
	VD (n = 79)	10.74[b] ± 2.92	1.57 ± 0.23	—	—
	CCHB (n = 70)	10.30[c] ± 2.51	1.03 ± 0.24	—	—
Canal flare index	CT, 0° (n = 79)	2.00[a] ± 0.30	—	—	—
	VD (n = 79)	1.54[b] ± 0.27	−0.45 ± 0.06	−0.161	19%
	CCHB (n = 70)	1.62[b] ± 0.26	−0.35 ± 0.07	0.331	23%
	CT, −10° (n = 79)†	1.99[a] ± 0.28	0.00 ± 0.02	—	—
	CT, −5° (n = 79)	1.99[a] ± 0.29	−0.01 ± 0.02	—	—
	CT, 0° (n = 79)	2.00[a,c] ± 0.30	—	—	—
	CT, +5° (n = 79)	2.01[b,c] ± 0.31	0.02 ± 0.02	—	—
	CT, +10° (n = 79)	2.03[b,d] ± 0.30	0.04 ± 0.02	—	—

*Bias, ICC, and accuracy referred to difference between radiographic views and CT. For radiographs, accuracy was defined as a canal flare index difference with CT < 0.2. †Negative angles represent external rotation of the femur relative to the radiographic beam.

— = Not applicable. CCHB = Craniocaudal horizontal beam radiographic view. ICC = Intraclass correlation coefficient. VD = Ventrodorsal radiographic view.

[a–d]For comparisons among the 3 viewing methods and for comparisons among CT rendering orientations, mean values with different superscript letters differ statistically among methods or orientations ($P < .05$).

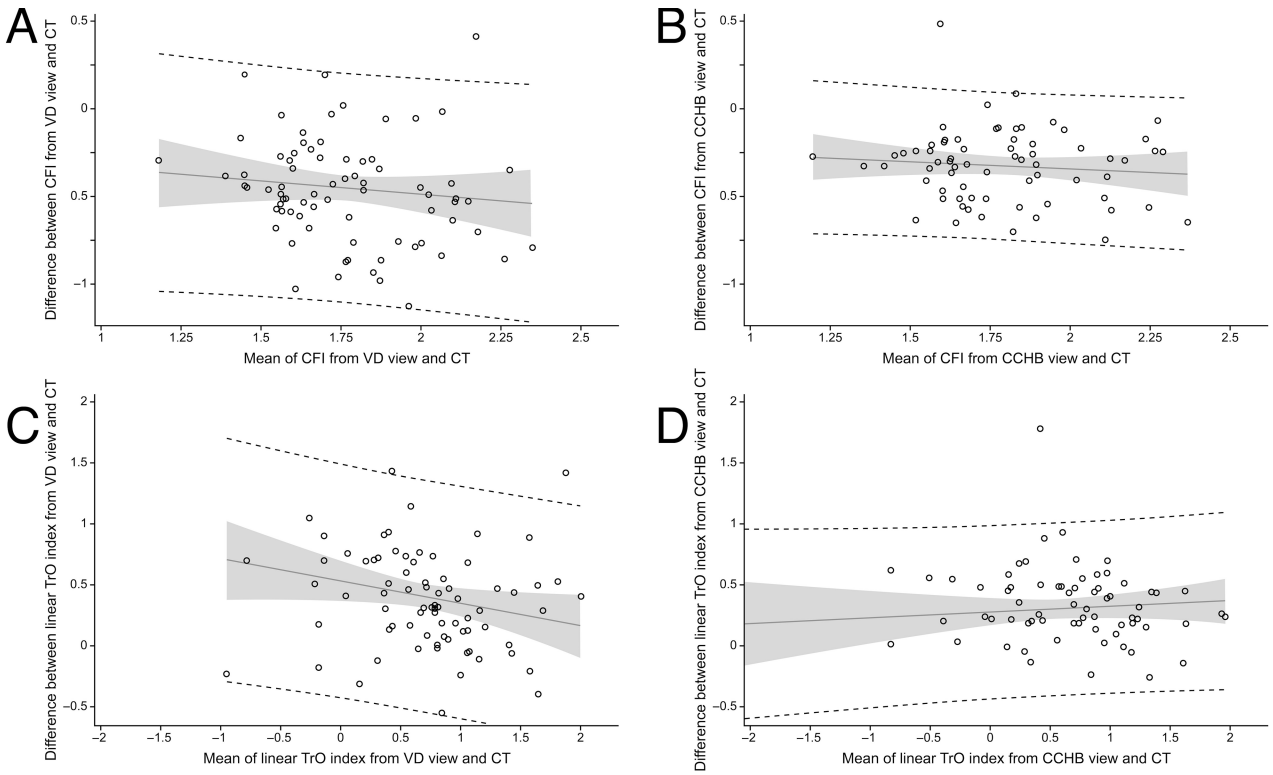

Figure 3—Bland-Altman plots (average of radiographic view scores and CT-derived scores for CFI and linear TrO index vs the difference between radiographic view and CT-derived scores) of CFI and linear TrO index for the femurs described in the legend of Figure 1. The results are shown for 79 VD views and 70 CCHB views. Solid lines represent the regression line, shaded areas represent the 95% CI of the regression line, and dashed lines represent the 95% prediction limits. For the CFI, a negative bias of −0.45 was present on VD views (A) and −0.33 on CCHB views (B). For the linear TrO index, a positive bias of 0.40 was observed on VD views (C) and 0.30 on CCHB views (D).

Table 2—Trochanteric overhang (TrO) measurements from 2 radiographic views and from CT scans of 80 femurs from 43 dogs.

Parameter	Viewing method	Mean ± SD	Bias (limits of agreement)	ICC	Agreement (κ)	Accuracy*
Linear TrO index†	CT, 0° (n = 80)	0.51[a] ± 0.67	—	—	—	—
	VD (n = 78)	0.91[b] ± 0.58	0.40 ± 0.11	0.546	—	25%
	CCHB (n = 70)	0.77[b] ± 0.7	0.30 ± 0.11	0.771	—	26%
	CT, −10° (n = 80)	0.54[a] ± 0.70	0.03 ± 0.03	—	—	—
	CT, −5° (n = 80)	0.52[a] ± 0.68	0.02 ± 0.03	—	—	—
	CT, 0° (n = 80)	0.51[a] ± 0.67	—	—	—	—
	CT, +5° (n = 80)	0.49[b] ± 0.67	−0.01 ± 0.03	—	—	—
	CT, +10° (n = 80)	0.46[b] ± 0.66	−0.04 ± 0.03	—	—	—
TrO grade	CT, 0° (n = 80)	3[a] (1–4)‡	—	—	—	—
	VD (n = 78)	3[b] (1–4)‡	−0.39 ± 0.14	—	0.559	56%
	CCHB (n = 70)	3[b] (1–4)‡	−0.28 ± 0.14	—	0.679	70%
	CT, −10° (n = 80)	3[a] (1–4)‡	−0.01 ± 0.07	—	—	—
	CT, −5° (n = 80)	3[a] (1–4)‡	−0.03 ± 0.07	—	—	—
	CT, 0° (n = 80)	3[a] (1–4)‡	—	—	—	—
	CT, +5° (n = 80)	3[a,b] (2–4)‡	0.04 ± 0.07	—	—	—
	CT, +10° (n = 80)	3[b] (2–4)‡	0.09 ± 0.07	—	—	—
Volumetric TrO index	CT, 0° (n = 80)	0.63 ± 0.96	—	—	—	—

*For radiographs, accuracy was defined a TrO distance to the canal center differing from CT measurement > 20% of canal radius or having the same TrO grade. †The distance of the medial aspect of the greater trochanter to the mechanical axis in the frontal plane divided by the canal radius. Larger indices indicate less overhang. An index ≥ 1 indicates no overhang. ‡Median (range).

— = Not applicable.

[a,b]For comparisons among the 3 viewing methods and for comparisons among CT rendering orientations, mean values with different superscript letters differ statistically among methods or orientations ($P < .05$).

joints with hip dysplasia, 4 femurs had a femoral head fracture, 2 were chronically luxated, and 8 were normal. The median age was 26 months (range, 5 to 121). The mean ± SD bodyweight was 28.2 ± 10.4 kg (range, 9.7 to 53.0). Five dogs weighed < 15 kg and 11 weighed < 20 kg. The dogs included 18 spayed females (42%), 14 neutered males (33%), 9 intact males (21%), and 2 intact females (5%). Multiple breeds were included; among those were 11 mixed-breed dogs and 10 German Shepherd dogs. The mean ± SD OA score was 20 ± 11 and subluxation index was 86% ± 48%.

Measurements of CFI were collected from 79 VD views, 70 CCHB views, and 79 CT renderings **(Table 1)**. One VD view and 10 CCHB views were not available. Relative to CT measurements, measurements from VD and CCHB radiographic views underestimated endosteal width and overestimated diaphyseal width at the femoral isthmus (all P < .001). Radiographic views underestimated CFI relative to CT measurements, with a mean bias (± limits of agreement) of −0.45 ± 0.06 for the VD view (P < .001) and −0.35 ± 0.07 for the CCHB view (P = .002; **Figure 3**). Eighty-one percent of VD views and 77% of CCHB views inaccurately measured CFI by > 0.2. The VD and CCHB radiographic views had poor consistency relative to CT measurements (ICC, −0.161 and 0.331, respectively). Factors influencing the correlation between radiographic and CT measurements of CFI were not identified. Mean measurements of CFI were 0.04 greater when femurs were internally rotated by 10° compared to nonrotated femurs (P = .011). Mean CFI measurements for other femoral rotations did not differ statistically from measurements in nonrotated femurs (P values ranging from .057 to .416). Bodyweight was not associated with the CFI measured on VD and CCHB views and on CT scans (P values ranging from .306 to .915).

Measurements of TrO were collected from 78 VD views, 70 CCHB views, and 80 CT renderings **(Table 2)**. Two VD views were not used: 1 was not available, and 1 was incomplete. Ten CCHB views were not available. Radiographic views overestimated the linear TrO index, with a mean bias (± limit of agreement) relative to CT measurements of 0.40 ± 0.11 for the VD view and 0.30 ± 0.11 for the CCHB view. The error in TrO location relative to the canal center was > 20% of the canal radius in 75% of VD views and 74% of CCHB views. Measurements of linear TrO index from VD views had moderate consistency relative to CT measurements (ICC, 0.546), and measurements from CCHB views had good consistency (ICC, 0.771). Larger diaphyseal width was significantly associated with a larger bias of linear TrO index between CCHB view and CT (r^2 = 0.058; P = .045). Other factors influencing the correlation between radiographic and CT measurements of TrO were not identified. Mean measurements of linear TrO index were 0.04 lower when femurs were internally rotated by 10° compared to nonrotated femurs (P = .019). Mean TrO measurements for other femoral rotations did not differ statistically from measurements in nonrotated femurs (P values ranging from .052 to .415).

Radiographic views also underestimated TrO grade, with a mean (± limit of agreement) TrO grade bias relative to CT measurements of −0.39 ± 0.14 for the VD view and −0.28 ± 0.14 for the CCHB view. Measurements of TrO grade from VD views had moderate agreement with CT measurements (κ = 0.559), and measurements of CCHB views had substantial agreement with CT measurements (κ = 0.679). Compared to CT grades, radiographic grades of TrO were incorrect in 44% of VD views and 30% of CCHB views. Factors influencing the correlation of

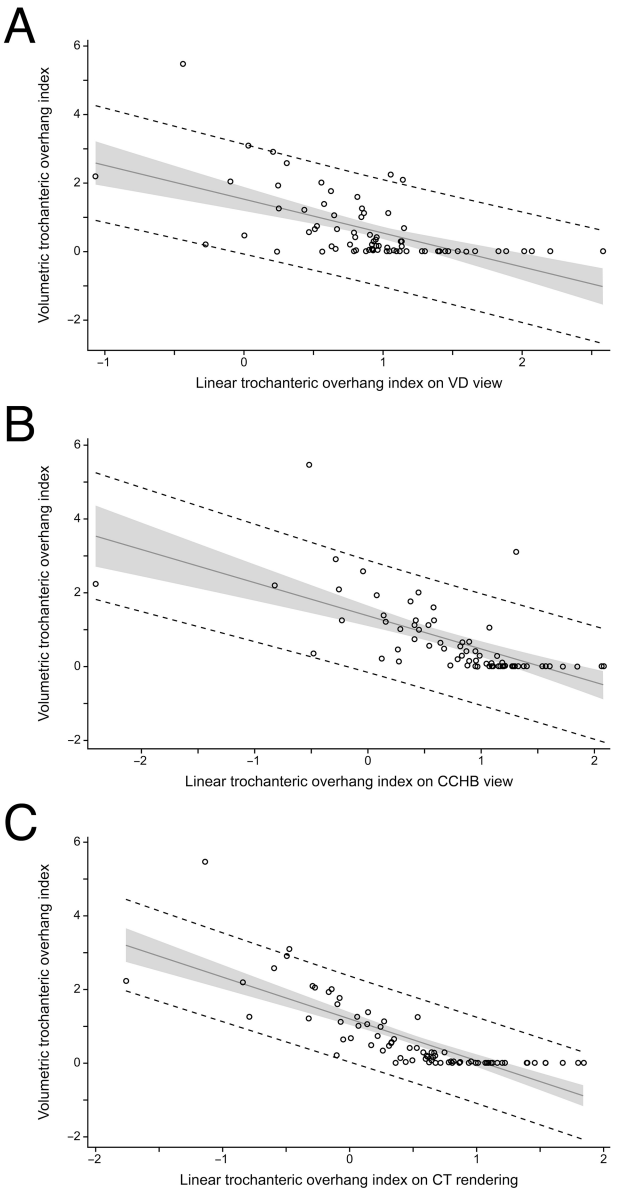

Figure 4—Linear regression plots showing TrO from the 80 femurs from 43 dogs described in the legend of Figure 1. The plots compared linear measurements of TrO index from VD radiographic views (A), CCHB radiographic views (B), and CT-derived renderings (C) to normalized volumetric TrO. For all linear measurements of TrO index, measurements ≥ 1 represent no overhang. Regression lines are gray, and their 95% CIs are shaded. Dashed lines represent the 95% prediction limits for TrO.

TrO grades for radiographic views and CT renderings were not identified. Mean measurements of TrO grade were 0.09 greater when femurs were internally rotated by 10° compared to nonrotated femurs (P = .019). Mean measurements of TrO grade for other rotated femurs did not differ statistically from nonrotated femurs (P values ranging from .313 to .720). Bodyweight was not associated with the linear TrO index measured on VD and CCHB views and on CT scans (P values ranging from .450 to .884).

When evaluating TrO volumetrically, 22 of 80 femurs (28%) had no TrO. The medial aspect of the greater trochanter was cranial to the proximal extension of the canal in 12 femurs (15%), was within the canal in 30 femurs (38%), and was caudal in 16 femurs (20%; Figure 2). Linear measurements of TrO index and TrO grades from VD views (r^2 = 0.330 and 0.355, respectively), CCHB views (r^2 = 0.422 and 0.384), and CT renderings (r^2 = 0.637 and 0.472) were significantly correlated with volumetric measurements of TrO index (all P values < .001; **Figure 4**). The slope of the regression line for CT renderings differed statistically from the slope of the regression line for TrO grades from VD views (P = .033) but not from other regression lines (P values ranging from .088 to .809).

Discussion

Reconstructions of CT scans were used as references in this study because they are not sensitive to parallax, distortion, or magnification.[23,24] Computer-aided design software was used to virtually sketch the proximal portion of the femur at its frontal plane midsection, to mark anatomic landmarks used to calculate CFI and TrO, and to project these landmarks on a virtual sketch, maximizing the accuracy of CFI and linear TrO index calculations. The mean CT measurements of CFI observed in the current study were similar to the anatomic measurements of CFI reported in previous studies[25,26] (2.00 to 2.10). To control for dog size, linear measurements of TrO were indexed by dividing by the radius of the canal. The volume of greater trochanter overhanging proximal to the canal was calculated as removal of overhanging bone during THR stem placement is commonly performed to maximize canal fill and optimize stem alignment. The location of the medial aspect of the greater trochanter relative to the canal in the transverse plane was recorded because a portion of the overhanging trochanter could be located cranial or caudal to the canal, decreasing the amount of bone overhanging the canal.

The VD and CCHB radiographic views underestimated canal flare. We accepted the hypothesis that measurements of CFI from VD and CCHB views are inaccurate. Radiographic underestimation of CFI was caused by overestimation of diaphyseal width, due to magnification of the femoral diaphysis secondary to the lack of hip extension, and by underestimation of endosteal width at the lesser trochanter, possibly due to superimposition of cortical bone.[13] These errors were numerically smaller for CCHB views than for VD views as found in a previous study.[26] We accepted the hypothesis that CCHB views were more accurate than VD views. This is because femurs are more perpendicular to the radiographic beam and more parallel to the cassette on CCHB views than on VD views, decreasing femoral parallax and distortion. An attempt was made to position the x-ray beam consistently. It is possible that a more precise position of the x-ray beam at the midpoint between the lesser trochanter and anticipated femoral isthmus would have decreased parallax and increased the accuracy of CFI measurements. In previous studies[23,27] in dogs, a lack of hip extension on radiographic views led to femoral foreshortening and influenced geometric measurements. The size of the difference between radiographic and CT measurements of CFI in the current study was surprisingly large. An error in CFI of 0.45 (the bias identified in this study for VD views) would lead to a misinterpretation of a femur with a true CFI of 2.15 (a normal femur, with CFI > 1.8 and ≤ 2.4) to a perceived CFI of 1.70 (a stovepipe femur, with CFI ≤ 1.8),[12] potentially influencing the surgeon's recommendations.[28] A negative bias for radiographic measurements of CFI was also observed in a study comparing VD and CCHB radiographic measurements to anatomic measurements.[26] However, in that study, the bias between radiographic and anatomic CFI measurements was only 0.1. The source of the difference between these biases is not known. While both anatomic and CT-based measurements of CFI would likely be accurate,[29] they may differ slightly. Radiographic measurements of CFI in the anatomic study may have been greater than measurements in the current study because they were collected from cadavers with normal hip joints instead of dogs with hip dysplasia. In the literature, mean radiographic measurements of CFI are greater in dogs with normal hip joints (2.09 to 2.73)[25,30–32] than in dogs undergoing THR (1.57 to 1.98).[14–16] Also, the breed distribution may have differed among studies. Breed-specific CFIs have been shown to vary widely.[12,16,32–35] In the current study, the severity of OA did not have a statistical impact of the accuracy of radiographic measurements of CFI. This is most likely because OA changes are concentrated around the femoral head, femoral neck, and acetabulum rather than on the lesser trochanter and diaphysis. We rejected the hypothesis that the severity of OA influences the accuracy of CFI assessment.

Trochanteric overhang has been associated with varus orientation of the prosthetic stem in both canine and human THR.[11,36,37] While TrO has a clear impact on THR in dogs, the peer-reviewed literature describing TrO is scant.[10,11] A volumetric measure of TrO was developed to determine the actual amount of trochanteric bone that would be in the path of instruments and implants during cementless THR. Based on correlation analysis, linear measurements of TrO were consistent with volumetric measurements of TrO, particularly for the CCHB radiographic view. Therefore, TrO measurements from radiographs can be used to reasonably predict the overhanging trochanteric volume. When the position of the medial aspect of the greater trochanter was evaluated in the transverse plane, that position varied widely. The medial aspect of the greater trochanter was

lateral to the proximal extension of the canal in < 30% of the femurs, meaning that more than 2 thirds of the femurs in the current study had TrO. The medial aspect of the greater trochanter was within the proximal extension of the canal in approximately a third of femurs and was cranial or caudal to the proximal extension of the canal in more than a third of femurs. The cranial or caudal position of the medial aspect of the greater trochanter relative to the canal was likely associated with femoral torsion. Cranial displacement of the greater trochanter most likely resulted from external torsion of the femur, and, conversely, caudal displacement resulted from internal torsion. Femoral torsion varies widely among dogs. In 2 studies,[29,38] the range of femoral torsion was approximately 30°. The wide range in the position of the medial aspect of the greater trochanter is similar to a finding in a sample of human femurs, where trochanteric anteversion (the position of the greater trochanter relative to the anatomic axis of the femur in the transverse plane) varied from 17° to 73°.[39] The variable position of the greater trochanter relative to the canal suggests that the radiographic assessment of TrO should include the assessment of the position of the greater trochanter relative to the mechanical axis of the proximal portion of the femur in the sagittal plane in addition to the frontal plane. That evaluation can be based on an open-leg lateral view of the femur or a lateral view of the pelvis. On VD and CCHB views acquired with a cranial view of the stifle joint, a cranially or caudally located greater trochanter would appear to be overhanging the canal. On open-leg lateral or lateral views acquired with the femoral condyles superimposed, the location of the greater trochanter cranial or caudal to the canal can be detected. The evaluation of the trochanteric position in the sagittal plane, however, can be challenging because of partial superimposition with the femoral head, femoral neck, and acetabulum.[40]

The VD and CCHB radiographic views underestimated TrO in the frontal plane. When considering the sagittal plane, however, the VD and CCHB radiographic overestimated TrO because the medial aspect of the greater trochanter was not always located within the proximal extension of the medullary canal. The medial aspect of the greater trochanter was outside the proximal extension of the medullary canal in 35% of femurs: cranial in 15% of femurs and caudal in 20% of femurs. When the medial aspect of the greater trochanter was outside the proximal extension of the medullary canal, the TrO observed on radiographs overestimated the true TrO. We accepted the hypothesis that measurements of TrO from VD and CCHB views are inaccurate. Subjectively, the underestimation of TrO in the frontal plane was only marginally smaller on CCHB views than on VD views, suggesting that TrO underestimation did not solely result from foreshortening of the femur. Underestimation of TrO may have been due to the errors in capture of the orientation of the lateral cortical and endosteal surfaces and the femoral long axis. Small errors in femoral shaft alignment were observed in 2 studies[23,41] comparing CT and radiographic measurements. The source of the greater linear TrO index error (bias) present in larger dogs compared to smaller dogs is not known. Since an association between bodyweight and linear TrO index was not identified on radiographs or CT, geometric differences among femurs from smaller and larger dogs were unlikely. Possibly, a difference was not identified because relatively few small dogs were included in the study. Positioning larger dogs for radiographs was likely more challenging than positioning smaller dogs, potentially increasing positioning errors in large dogs. In the current study, the TrO grades calculated from radiographic views using the previously reported TrO grading scheme[11] differed from grades calculated from CT renderings in nearly half of the VD views and in nearly a third of CCHB views. This suggests that further research is warranted to more accurately characterize TrO based on radiographic views. The severity of OA did not have a statistical impact on the accuracy of radiographic measurements of TrO. This is most likely because OA changes only marginally impact the greater trochanter. We rejected the hypothesis that the severity of OA and subluxation influence the accuracy of TrO assessment.

We accepted the hypothesis that femoral internal rotation of 10° decreases the accuracy of radiographic assessment of CFI and TrO. This finding is in agreement with several studies[42,43] that described inaccuracy in the geometric assessment of the canine femur resulting from rotational malpositioning. Differences in femoral rotation on radiographs and CT renderings were a possible source of inaccuracy of CFI and TrO measurements. Potential differences in rotational position between radiographic views and CT renderings, however, were minimized by orienting radiographs and CT renderings similarly and consistently so that all projections approximated true craniocaudal views of the distal portion of the femur. In 3-D femoral geometry studies,[18,44] the frontal plane is based on the axis joining the center of the medial and lateral femoral condyles or the axis joining the caudal aspect of the medial and lateral condyles.[23,45,46]

The current study had limitations. The radiographic views evaluated did not include the caudocranial femoral view, sometimes used to plan THR.[2,41] Canal flare was calculated using a single method, dividing endosteal width at the proximodistal midpoint of the lesser trochanter by the width at the isthmus.[12] The isthmus is approximately located at the distal aspect of the proximal third of the femur, and its position varies slightly among dogs.[31] Alternative canal flare measurement methods that use the endosteal width at the proximal aspect of the lesser trochanter or the diaphyseal width at the proximodistal femoral midpoint have been used to calculate canal flare,[14,33,35] yielding differences in CFI comparable to those in the current study.[25] Canal flare and TrO could have been evaluated using technically simpler CT methods, such as multiplanar reconstruction or maximum intensity projection.[45,47] Canal flare and TrO could also have been evaluated on CT renderings with other controlled malpositions, such as a lack of hip extension. For those analyses, distorted sketch projections of femurs with differential magnification

could have been prepared by adjusting perspective settings in the computer-aided design software. The accuracy thresholds of 0.2 for CFI and 20% of canal radius for TrO were selected to represent potentially clinically impactful errors. These thresholds were subjective. Volumetric TrO measurements were collected because they represent a more quantitative measure of overhang than the position of the medial aspect of the greater trochanter. The volume of overhanging bone likely estimates the technical difficulty of stem insertion during THR. However, the clinical impact of specific TrO on THR is not known. Several strategies, such as medializing the stem, altering stem anteversion, and selective rasping, may decrease the impact of TrO during the implantation of a press-fit stem. The presence of TrO also complicates the implantation of stems stabilized using bolts and screws. The clinical impact of the errors in measurements of CFI and TrO identified in the current study is unknown. Presumably, underestimating CFI would lead to an overestimation of the proportion of dogs deemed to have stovepipe femurs, potentially leading clinicians to implant more cemented stems.[28] Underestimating TrO could lead to the implantation of undersized stems or to underestimation of the proportion of femurs requiring trochanteric rasping during THR to insert a stem without varus angulation.[10,48] Future research could focus on evaluating the risks of subsidence, fracture, or lack of bone ingrowth associated with the implantation of specific cementless stems in bones with varying CFIs and to evaluate safe and effective strategies to insert stems axially into femurs with TrO, including trochanteric osteotomies.[49]

We concluded that measurements of CFI and TrO from VD views, and, to a lesser extent, from CCHB views, are inaccurate relative to CT measurements. We also concluded that internal femoral rotation of 10° decreases the accuracy of radiographic assessment of CFI and TrO. The use of a CT scan of the femur to evaluate canal flare and TrO should be considered when measurements must be accurate and when planning THR in patients with femoral deformities.

Acknowledgments

The authors thank Chrisoula Toupadakis Skouritakis, PhD, University of California-Davis, for the illustrations.

Disclosures

Dr. Marcellin-Little is a member of the *AJVR* Scientific Review Board, but was not involved in the editorial evaluation of or decision to accept this article for publication.

No AI-assisted technologies were used in the composition of this manuscript.

Funding

This study was funded by the Center for Companion Animal Health, University of California-Davis.

ORCID

D. J. Marcellin-Little https://orcid.org/0000-0001-6596-5928

References

1. Lascelles BD, Freire M, Roe SC, DePuy V, Smith E, Marcellin-Little DJ. Evaluation of functional outcome after BFX total hip replacement using a pressure sensitive walkway. *Vet Surg.* 2010;39(1):71–77. doi:10.1111/j.1532-950X.2009.00607.x
2. Kwok JY, Wendelburg KL. Clinical outcomes of canine total hip replacement utilizing a BFX lateral bolt femoral stem: 195 consecutive cases (2013-2019). *Vet Surg.* 2023;52(1):51–61. doi:10.1111/vsu.13871
3. Allaith S, Tucker LJ, Innes JF, et al. Outcomes and complications reported from a multiuser canine hip replacement registry over a 10-year period. *Vet Surg.* 2023;52(2):196–208. doi:10.1111/vsu.13885
4. Edwards MR, Egger EL, Schwarz PD. Aseptic loosening of the femoral implant after cemented total hip arthroplasty in dogs: 11 cases in 10 dogs (1991-1995). *J Am Vet Med Assoc.* 1997;211(5):580–586. doi:10.2460/javma.1997.211.05.580
5. Ota J, Cook JL, Lewis DD, et al. Short-term aseptic loosening of the femoral component in canine total hip replacement: effects of cementing technique on cement mantle grade. *Vet Surg.* 2005;34(4):345–352. doi:10.1111/j.1532-950X.2005.00053.x
6. Bergh MS, Gilley RS, Shofer FS, Kapatkin AS. Complications and radiographic findings following cemented total hip replacement: a retrospective evaluation of 97 dogs. *Vet Comp Orthop Traumatol.* 2006;19(3):172–179. doi:10.1055/s-0038-1632994
7. Ramamurti BS, Orr TE, Bragdon CR, Lowenstein JD, Jasty M, Harris WH. Factors influencing stability at the interface between a porous surface and cancellous bone: a finite element analysis of a canine in vivo micromotion experiment. *J Biomed Mater Res.* 1997;36(2):274–280. doi:10.1002/(sici)1097-4636(199708)36:2<274::aid-jbm17>3.0.co;2-g
8. Pernell RT, Milton JL, Gross RS, et al. The effects of implant orientation, canal fill, and implant fit on femoral strain patterns and implant stability during catastrophic testing of a canine cementless femoral prosthesis. *Vet Surg.* 1995;24(4):337–346. doi:10.1111/j.1532-950x.1995.tb01340.x
9. Pernell RT, Gross RS, Milton JL, et al. Femoral strain distribution and subsidence after physiological loading of a cementless canine femoral prosthesis: the effects of implant orientation, canal fill, and implant fit. *Vet Surg.* 1994;23(6):503–518. doi:10.1111/j.1532-950x.1994.tb00512.x
10. Silveira CJ, Saunders WB. Greater trochanter osteotomy as a component of cementless total hip replacement: five cases in four dogs. *Vet Surg.* 2022;51(2):303–310. doi:10.1111/vsu.13742
11. Silveira CJ, Barnes KH, Kerwin SC, Saunders WB. Greater trochanter morphology and association with patient demographics, surgical factors, and post-operative stem position: a retrospective assessment of 150 cementless THRs in 135 dogs. *BMC Vet Res.* 2022;18(1):78. doi:10.1186/s12917-022-03174-y
12. Rashmir-Raven AM, DeYoung DJ, Abrams CF Jr, Aberman HA, Richardson DC. Subsidence of an uncemented canine femoral stem. *Vet Surg.* 1992;21(5):327–331. doi:10.1111/j.1532-950x.1992.tb01705.x
13. Stevens PM. Radiographic distortion of bones: a marker study. *Orthopedics.* 1989;12(11):1457–1463. doi:10.3928/0147-7447-19891101-11
14. Ganz SM, Jackson J, VanEnkevort B. Risk factors for femoral fracture after canine press-fit cementless total hip arthroplasty. *Vet Surg.* 2010;39(6):688–695. doi:10.1111/j.1532-950X.2010.00694.x
15. Marcellin-Little DJ, DeYoung BA, Doyens DH, DeYoung DJ. Canine uncemented porous-coated anatomic total hip arthroplasty: results of a long-term prospective evaluation of 50 consecutive cases. *Vet Surg.* 1999;28(1):10–20. doi:10.1053/jvet.1999.0010
16. Pugliese LC. Proximal femoral morphology and bone quality assessment in dogs: Master's thesis. The Ohio State University; 2014.
17. Enomoto M, Baines EA, Roe SC, Marcellin-Little DJ, Lascelles BDX. Defining the rate of, and factors influencing,

radiographic progression of osteoarthritis of the canine hip joint. *Vet Rec.* 2021;189(10):e516.
18. Savio G, Baroni T, Concheri G, et al. Computation of femoral canine morphometric parameters in three-dimensional geometrical models. *Vet Surg.* 2016;45(8):987–995. doi:10.1111/vsu.12550
19. Shrout PE, Fleiss JL. Intraclass correlations: uses in assessing rater reliability. *Psychol Bull.* 1979;86(2):420–427. doi:10.1037/0033-2909.86.2.420
20. Portney LG. *Foundations of Clinical Research: Applications to Evidence-Based Practice.* Prentice Hall; 2020.
21. Landis JR, Koch GG. The measurement of observer agreement for categorical data. *Biometrics.* 1977;33(1):159–174. doi:10.2307/2529310
22. Bland JM, Altman DG. Agreement between methods of measurement with multiple observations per individual. *J Biopharm Stat.* 2007;17(4):571–582. doi:10.1080/10543400701329422
23. Brühschwein A, Schmitz B, Zöllner M, Reese S, Meyer-Lindenberg A. Introduction of a bone-centered three-dimensional coordinate system enables computed tomographic canine femoral angle measurements independent of positioning. *Front Vet Sci.* 2022;9:1019215. doi:10.3389/fvets.2022.1019215
24. Fitzwater KL, Marcellin-Little DJ, Harrysson OL, Osborne JA, Poindexter EC. Evaluation of the effect of computed tomography scan protocols and freeform fabrication methods on bone biomodel accuracy. *Am J Vet Res.* 2011;72(9):1178–1185. doi:10.2460/ajvr.72.9.1178
25. Sevil-Kilimci F, Kara ME. Canal flare index in the canine femur is influenced by the measurement method. *Vet Comp Orthop Traumatol.* 2020;33(3):198–204. doi:10.1055/s-0040-1701501
26. de Andrade CR, Minto BW, Dreibi RM, et al. Accuracy in determining canal flare index using different radiographical positions for imaging canine femurs. *Vet Comp Orthop Traumatol.* 2019;32(3):234–240. doi:10.1055/s-0039-1683390
27. Maguire P, Siclari M, Lesser A. Femoral imaging artifacts associated with dorsal recumbency craniocaudal radiographic positioning: description of a modified bisecting angle technique. *Vet Comp Orthop Traumatol.* 2014;27(4):288–296. doi:10.3415/VCOT-13-10-0129
28. Meltzer LM, Dyce J, Leasure CS, Canapp SO Jr. Case factors for selection of femoral component type in canine hip arthroplasty using a modular system. *Vet Surg.* 2022;51(1):286–295. doi:10.1111/vsu.13752
29. Dudley RM, Kowaleski MP, Drost WT, Dyce J. Radiographic and computed tomographic determination of femoral varus and torsion in the dog. *Vet Radiol Ultrasound.* 2006;47(6):546–552. doi:10.1111/j.1740-8261.2006.00184.x
30. Palierne S, Asimus E, Mathon D, Meynaud-Collard P, Autefage A. Geometric analysis of the proximal femur in a diverse sample of dogs. *Res Vet Sci.* 2006;80(3):243–252. doi:10.1016/j.rvsc.2005.07.010
31. Palierne S, Mathon D, Asimus E, Concordet D, Meynaud-Collard P, Autefage A. Segmentation of the canine population in different femoral morphological groups. *Res Vet Sci.* 2008;85(3):407–417. doi:10.1016/j.rvsc.2008.02.010
32. Christopher SA, Kim SE, Roe S, Pozzi A. Biomechanical evaluation of adjunctive cerclage wire fixation for the prevention of periprosthetic femur fractures using cementless press-fit total hip replacement. *Vet J.* 2016;214:7–9. doi:10.1016/j.tvjl.2016.04.014
33. Sevil-Kilimci F, Kara ME. The geometry of the proximal femoral medullary canal in German Shepherd and Kangal dogs. *J Fac Vet Med Istanbul Univ.* 2017;43:52–60. doi:10.16988/iuvfd.270288
34. Kemp TJ, Bachus KN, Nairn JA, et al. Functional trade-offs in the limb bones of dogs selected for running versus fighting. *J Exp Biol.* 2005;208(pt 18):3475–3482. doi:10.1242/jeb.01814
35. Gomide PRS, de Souza LRV, de Andrade CR, Dreibi RM, Santarosa BP, Minto B. Canal flare index evaluation for different dog breeds. *Ciência Rural Santa Maria.* 2021;51(4):e20200068. doi:10.1590/0103-8478cr20200068
36. Bayley M, Cnudde P, Adds PJ, Jones S, Williams RL. Does medial overhang of the greater trochanter influence femoral stem position during cemented hip arthroplasty? A retrospective radiological review. *Cureus.* 2020;12(10):e10968.
37. Horberg JV, Tapscott DC, Kurcz BP, et al. Morphology of the greater trochanter: an assessment of anatomic variation and canal overhang. *Arthroplast Today.* 2020;6(4):644–649. doi:10.1016/j.artd.2020.07.020
38. Nunamaker DM, Biery DN, Newton CD. Femoral neck anteversion in the dog: its radiographic measurement. *Vet Radiol.* 1973;14(1):45–48. doi:10.1111/j.1740-8261.1973.tb00647.x
39. Gulledge BM, Marcellin-Little DJ, Levine D, et al. Comparison of two stretching methods and optimization of stretching protocol for the piriformis muscle. *Med Eng Phys.* 2014;36(6):212–218. doi:10.1016/j.medengphy.2013.10.016
40. Forzisi I, Vezzoni A, Vezzoni L, Drudi D, Bourbos A, Marcellin-Little DJ. Evaluation of the effects of cementless total hip replacement on femoral length in skeletally immature dogs. *Vet Surg.* 2024;54(1):199–207. doi:10.1111/vsu.14180
41. Clark EA, Condon AM, Ogden DM, Bright SR. Accuracy of caudocranial canine femoral radiographs compared to computed tomography multiplanar reconstructions for measurement of anatomic lateral distal femoral angle. *Vet Comp Orthop Traumatol.* 2023;36(3):157–162. doi:10.1055/s-0043-1761242
42. Brand KJ, Beale BS, Hudson CC. Evaluation of a novel method to calculate cementless femoral stem level on craniocaudal projection radiographs. *Vet Surg.* 2021;50(8):1592–1599. doi:10.1111/vsu.13723
43. Frame EM, Breit S, Mayrhofer E. The canine trochanteric fossa: a radiographic and anatomic study. *Vet Radiol Ultrasound.* 2001;42(4):297–304. doi:10.1111/j.1740-8261.2001.tb00943.x
44. Hijikata H, Tanifuji O, Mochizuki T, et al. The morphology of the femoral posterior condyle affects the external rotation of the femur. *J Exp Orthop.* 2023;10(1):122. doi:10.1186/s40634-023-00686-w
45. Lusetti F, Bonardi A, Eid C, Brandstetter de Belesini A, Martini FM. Pelvic limb alignment measured by computed tomography in purebred English Bulldogs with medial patellar luxation. *Vet Comp Orthop Traumatol.* 2017;30(3):200–208. doi:10.3415/VCOT-16-07-0116
46. Longo F, Nicetto T, Banzato T, et al. Automated computation of femoral angles in dogs from three-dimensional computed tomography reconstructions: comparison with manual techniques. *Vet J.* 2018;232:6–12. doi:10.1016/j.tvjl.2017.11.014
47. Burg-Personnaz J, Zöllner M, Reese S, Meyer-Lindenberg A, Brühschwein A. 3D Slicer open-source software plug-in for vector-based angle calculation of canine hind limb alignment in computed tomographic images. *PLoS One.* 2024;19(3):e0283823. doi:10.1371/journal.pone.0283823
48. Tardiani L, Goldsmid S, Lanz O. Approach to the canine coxofemoral joint using an osteotomy of the deep gluteal muscle insertion for total hip replacements. *Front Vet Sci.* 2023;10:1224944. doi:10.3389/fvets.2023.1224944
49. Vaananen SP, Jurvelin JS, Isaksson H. Estimation of 3D shape, internal density and mechanics of proximal femur by combining bone mineral density images with shape and density templates. *Biomech Model Mechanobiol.* 2012;11(6):791–800. doi:10.1007/s10237-011-0352-9